Optical conductivity of bismuth-based topological insulators

P. Di Pietro, F. M. Vitucci, D. Nicoletti, L. Baldassarre, P. Calvani, R. Cava, Y. S. Hor, U. Schade, and S. Lupi

Phys. Rev. B **86**, 045439 — Published 24 July 2012

DOI: 10.1103/PhysRevB.86.045439

Optical conductivity of Bismuth-based topological insulators

P. Di Pietro[1], F. M. Vitucci[1], D. Nicoletti[2], L. Baldassarre[3], P. Calvani[1], R. Cava[4], Y.S. Hor[4], U. Schade[5] and S. Lupi[6]
[1] *CNR-SPIN and Dipartimento di Fisica, Università di Roma "La Sapienza", Piazzale A. Moro 2, I-00185 Roma, Italy*
[2] *Max Planck Research Department for Structural Dynamics Center for Free Electron Laser Science & University of Hamburg, Notkestrasse 85 - 22607 Hamburg, Germany*
[3] *Sincrotrone Trieste, Area Science Park, I-34012 Trieste, Italy*
[4] *Department of Chemistry, Princeton University, New Jersey 08544, U.S.A.*
[5] *Berliner Elektronenspeicherring-Gesellshaft für Synchrotronstrahlung m.b.H., Albert-Einstein Strasse 15, D-12489 Berlin, Germany and*
[6] *CNR-IOM, and Dipartimento di Fisica, Università di Roma "La Sapienza", Piazzale A. Moro 2, I-00185 Roma, Italy*
(Dated: July 10, 2012)

The optical conductivity $\sigma_1(\omega)$ and the spectral weight SW of four topological insulators with increasing chemical compensation (Bi_2Se_3, Bi_2Se_2Te, $Bi_{2-x}Ca_xSe_3$, Bi_2Te_2Se) have been measured from 5 to 300 K and from sub-THz to visible frequencies. The effect of compensation is clearly observed in the infrared spectra, through the suppression of an extrinsic Drude term and the appearance of strong absorption peaks, that we assign to electronic transitions among localized states. From the far-infrared spectral weight SW of the most compensated sample (Bi_2Te_2Se) one can estimate a density of charge-carriers in the order of $10^{17}/cm^3$ in good agreement with transport data. Those results demonstrate that the low-energy electrodynamics in single crystals of topological insulators, even at the highest degree of compensation presently achieved, is still influenced by 3D charge excitations.

PACS numbers: 78.30.-j, 78.20.Ci,71.55.-i,73.25.+i

INTRODUCTION

Topological Insulators (TI) are new quantum materials with an insulating gap in the bulk, of spin-orbit origin, and metallic states at the surface.[1–3] These states are chiral and show transport properties protected from back-scattering by the time-reversal symmetry. In addition to their fundamental properties, like exotic superconductivity [4, 5] and *axionic* eletromagnetic response, [6, 7] TI have potential applications in quantum computing,[8, 9]THz detectors [10] and spintronic devices.[11] After the discovery of a topological behavior in three-dimensional (3D) Bi_xSb_{1-x},[12] Bi_2Se_3 recently emerged, thanks to its large bulk insulating gap (E_G ∼300 meV), as the best candidate for the study of topological surface states.[13] In fact, Dirac quasiparticles (DQP) related to the topological surface states have been detected through Angle Resolved Photoemission Spectroscopy (ARPES) in Bi_2Se_3, Bi_2Te_3 and in their alloys Bi_2Se_2Te and Bi_2Te_2Se.[12, 14] Investigating the charge transport and cyclotron resonances of DQP has, however, proven to be challenging, because the surface current contribution is usually obscured by the extrinsic bulk carriers response.[15–17]

Indeed, as-grown crystals of Bi_2Se_3 display a finite density of Se vacancies which act as electron donors. They pin the bulk chemical potential μ_b within the conduction band thus producing, over a wide range of carrier concentrations, extrinsic n-type degenerate semiconducting behavior. Se vacancies also affect the low-energy transport properties of those materials,[18] making it difficult to distinguish the intrinsic metallic behavior due to the topological surface state from the extrinsic metallic conduction induced by the Se non-stoichiometry. As a consequence, both transport and optical conductivity experiments [16, 19] show a metallic behavior with a Drude term confined at low frequencies ($\omega < 600$ cm^{-1}) which mirrors the extrinsic carrier content. Two phonon peaks interacting with the electronic continuum have been observed in the far-infrared (FIR) range near 61 cm^{-1} (α mode) and 133 cm^{-1} (β mode).[16, 20] The bulk insulating gap instead spans between 250-350 meV, depending on the Se vacancy content, in good agreement with theoretical calculations.[21] At variance with Bi_2Se_3, single crystals of Bi_2Te_3 display p-type conductivity related to an excess of Bi atoms acting as acceptor centers.[15] These shift μ_b into the valence band so that, like for Bi_2Se_3, an extrinsic Drude term is observed in the FIR (here below $\omega < 400$ cm^{-1}).[22]

Motivated by the above observations, different authors adopted specific strategies to reduce the non-stoichiometry-induced bulk carriers in Bi_2Se_3 (Bi_2Te_3) materials. Hor *et al.* showed that Ca-doping in the Bi site ($Bi_{2-x}Ca_xSe_3$) progressively shifts μ_b from the conduction band to the valence band, thus changing as-grown n-type Bi_2Se_3 into a p-type degenerate semiconductor.[18] By exploiting the different doping chemistry of Bi_2Se_3 (n-type) and Bi_2Te_3 (p-type), a better compensation was obtained in the Bi_2Se_2Te and Bi_2Te_2Se alloys.[23, 24] In both systems a high resistivity at low T (exceeding 1 Ωcm) was observed at low T. Moreover, in Bi_2Se_2Te the variable range hopping (VRH) behavior expected for an impurity-driven conductivity was was found [23] to give place, below 20 K, to a T-independent σ_{dc}. This

crossover was reported as providing evidence that surface conductance prevails at low T in the best compensated system.[23]

However, as far as we know, the effects of chemical compensation have been not investigated on the optical properties of those materials. In this paper we fill this gap, by presenting the first optical data of four topological insulators - $Bi_{2-x}Ca_xSe_3$ ($x = 0$, 0.0002), Bi_2Se_2Te and Bi_2Te_2Se - from 5 to 300 K and from the sub-THz to the visible spectral range. The effects of the enhanced compensation are clearly visible in the FIR spectra, through the suppression of the Drude term and the appearance of strong absorption peaks that we assign to electronic transitions among localized states, similar to those found in weakly doped semiconductors. Our data show that the electrodynamics of Bi_2Te_2Se, *i. e.*, the most compensated sample, is still affected by 3D doped charges, as therein the FiR spectral weight is higher than the spectral weight associated with topological states by nearly two orders of magnitude.

EXPERIMENT

Single crystals with $x = 0$ were grown by a modified Bridgeman method, those of $Bi_{2-x}Ca_xSe_3$ via a process of two-step melting.[18] Chemical compensation (*i.e.* the insulating character) increases when passing from Bi_2Se_3 and Bi_2Se_2Te to $Bi_{2-x}Ca_xSe_3$ and Bi_2Te_2Se.[24] The basal (ab)-plane resistivity $\rho_{ab}(T)$ of the most compensated sample, Bi_2Te_2Se, shows an increasing (semiconducting) behavior down to about 50 K followed by a low-T regime in which resistivity saturates at values exceeding 1 Ωcm. In this regime, surface charge-carrier mobility much higher than the bulk mobility has been experimentally detected.[24, 25]

The reflectivity $R(\omega)$ of the four single crystals was measured at near-normal incidence with respect to the ab basal plane from sub-THz to visible frequencies at temperatures ranging from 5 to 300 K, shortly after cleaving the sample. The reference was obtained by *in-situ* evaporation of gold (silver) in the infrared (visible) range. In the sub-THz region (below 30 cm^{-1}) we used the Coherent Synchrotron Radiation (CSR) extracted from the electron storage ring BESSY II when working in the so-called *low-α* mode.[27] The real part of the optical conductivity $\sigma_1(\omega)$ was obtained from $R(\omega)$ via Kramers-Kronig transformations, after extrapolating $R(\omega)$ to zero frequency by Drude-Lorentz fits. The extrapolations to high frequency were based on data of Ref. 28.

RESULTS AND DISCUSSION

The reflectivity data for all samples are shown in Fig. 1. The FIR spectra in Figs. 1-a, -b are dominated by a free-carrier plasma edge around 500 cm^{-1} , which confirms the picture of an extrinsic electrodynamics in these materials. In $Bi_{1.9998}Ca_{0.0002}Se_3$ (Fig. 1-c), Ca doping shifts the plasma edge to about 400 cm^{-1}, while the strongest compensation is achieved in Bi_2Te_2Se (Fig. 1-d) where unshielded phonons are well resolved at 60 (α mode) and 130 (β mode) cm^{-1}. In all spectra a strong electronic absorption appears above 10000 cm^{-1}.

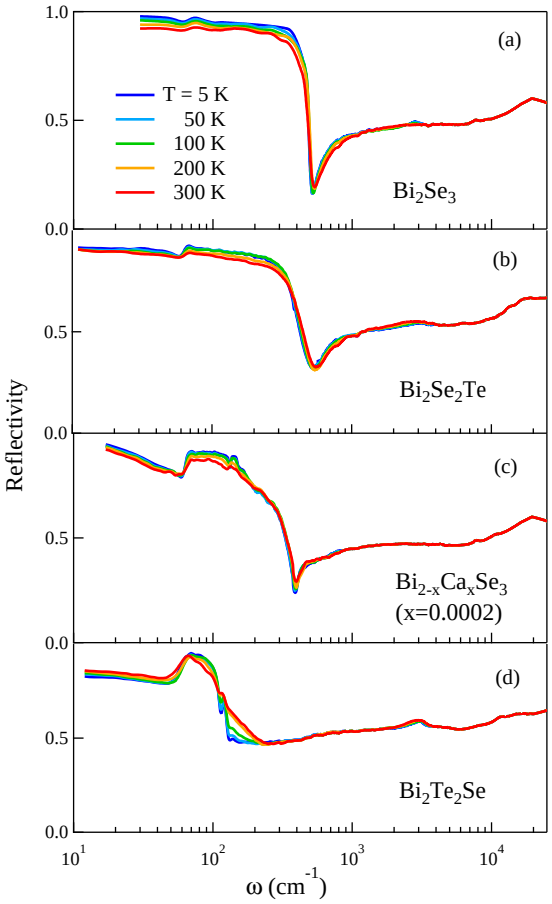

FIG. 1: (Color online) Reflectivity of Bi_2Se_3 (a), Bi_2Se_2Te (b), $Bi_{1.9998}Ca_{0.0002}Se_3$ (c) and Bi_2SeTe_2 (d) from 10 to 24000 cm^{-1} at different temperatures. The FIR spectra in a), b) (c) are characterized by a free-carrier plasma edge around 500 cm^{-1} (400 cm^{-1}), as well as phonon features α and β at about 60 and 130 cm^{-1} respectively. In d), due to a strong compensation (see text), the phonon absorptions can be clearer observed. In all spectra a weak bump develops at low-T around 3000 cm^{-1} corresponding to the direct-gap transition. The triplet direct gap appears instead above 10000 cm^{-1}.

The real part of the optical conductivity obtained from the $R(\omega)$ in Fig. 1 by Kramers-Kronig transformations is shown for the same temperatures and frequencies in Fig. 2. The direct gap transition, which corresponds to a small bump around 3000 cm^{-1} is barely visible due to its superposition with the huge triplet electronic exci-

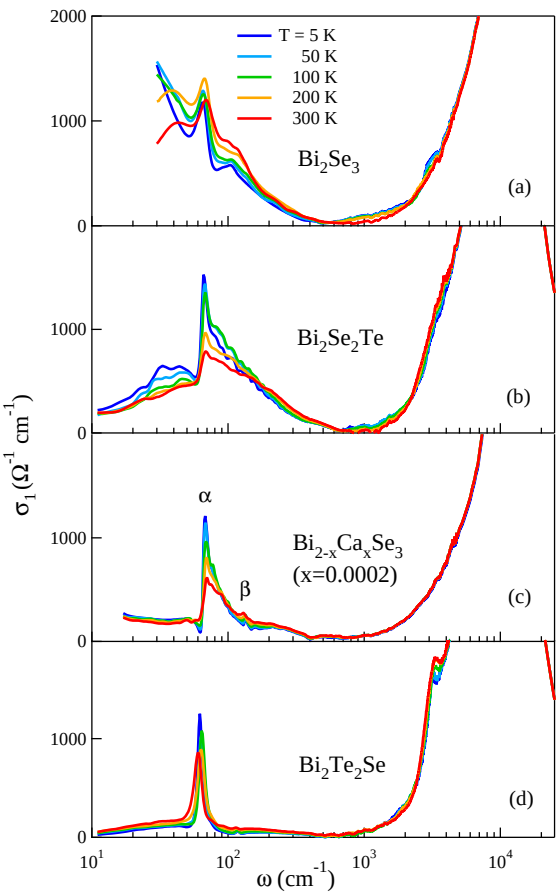

FIG. 2: (Color online) Real part of the optical conductivity of Bi_2Se_3 (a), Bi_2Se_2Te (b), $Bi_{1.9998}Ca_{0.0002}Se_3$ (c) and Bi_2SeTe_2 (d) from 10 to 24000 cm^{-1} at different temperatures. A broad minimum around 500 cm^{-1} separates the high-frequency interband transitions from the low-energy excitations. The α and β infrared-active phonon modes are indicated in panel (c).

tation present above 10000 cm^{-1}. These interband features, which will be not the focus of this paper, have been discussed in detail in Ref. 28. Most of the effects induced by compensation appears below 500 cm^{-1}. In particular, the most extrinsic system Bi_2Se_3 (Fig. 2-a), presents a Drude term superimposed to the α and β phonon peaks, which both sharpen for decreasing T. A similar behavior has been observed in Ref. 16 on a crystal with a comparable charge-carrier density ($\sim 10^{18}/cm^3$, see below). The effect of compensation becomes observable in Bi_2Se_2Te (Fig. 2-b). Here, at variance with an appreciable *dc* conductivity (σ_{dc} $\sim$200 Ω^{-1} cm^{-1},[26]) most of the FIR spectral weight is located at finite frequency in the phonon spectral region. A further drastic reduction of the spectral weight is finally obtained in $Bi_{1.9998}Ca_{0.0002}Se_3$ and Bi_2SeTe_2 (Figs. 2-c and -d).

The α phonon mode, both in Bi_2Se_2Te and $Bi_{1.9998}Ca_{0.0002}Se_3$, shows a Fano lineshape with a low frequency dip, more pronounced at low temperature. This suggests an interaction of this mode with an electronic continuum at lower frequency.[29] The Fano shape is much less evident in Bi_2Te_2Se, where the α phonon shows a nearly Lorentzian shape at room temperature and a weak low-frequency dip at low T. This indicates a transfer of the electronic continuum SW from above to below the phonon frequency for increasing temperature.[30] At variance with previous samples, the α mode in Bi_2Se_3 shows instead a high-frequency dip at all T's, in agreement with the observation reported in Ref. 16. This behavior suggests that the electronic-continuum is located in average at higher frequency with respect to the α-phonon characteristic frequency.

In order to better follow the evolution of both the lattice and the electronic optical conductivity, we have fitted to $\sigma_1(\omega)$ a Drude-Lorentz (D-L) model where the α phonon mode is described in terms of the Fano shape.[29] Examples of those fits (dotted lines) are shown in the insets of Fig. 3 at 5 K.

The $\sigma_1(\omega)$ in the FIR region, as obtained after subtraction of both interband and phonon contributions, is shown in the main panels of the same Figure. The electronic conductivity of Bi_2Se_3 (Fig. 3-a) can be described in terms of a Drude term (open circles) which narrows for decreasing T in agreement with the metallic behavior of the resistivity, [18] and of a broad absorption centered around 150 cm^{-1} (open squares). In Bi_2Se_2Te (Fig. 3-b) most of the FIR spectral weight is located in a broad band centered around 100 cm^{-1}. This band has been modeled through two Lorentzian contributions, peaked around 50 cm^{-1} (open triangles, FIR1) and 200 cm^{-1} (open squares, FIR2). In $Bi_{1.9998}Ca_{0.0002}Se_3$ the increased compensation results in an overall reduction of the FIR spectral weight. Moreover, the FIR absorption already observed in Bi_2Se_2Te (Fig. 3-b) splits into two bands: a narrow absorption centered at about 50 cm^{-1} and a broader one around 200 cm^{-1}. This double spectral structure is also achieved in Bi_2Te_2Se, where the low-frequency conductivity assumes a value comparable to the σ_{dc} $\sim$1 Ω^{-1} cm^{-1} measured in crystals belonging to the same batch.[24]

Similar low-frequency absorption bands have been observed in other, more conventional, doped semiconductors like Si:P.[31, 32] Therein, an insulator-to-metal transition (IMT) of Anderson type [33] can be observed for a charge-carrier density n_{IMT} $\sim$ 3.7 x $10^{18}/cm^3$.[31–33] Deeply inside the insulating phase ($n < n_{IMT}$), narrow peaks can be observed in the FIR conductivity corresponding to the hydrogen-like $1s \rightarrow np$ transitions of isolated P impurities. They are followed by a broad band at higher frequency, due to the transitions from the impurity bound states to the continuum. The narrow peaks broaden for increasing doping, giving rise to a low-frequency band which however remains dis-

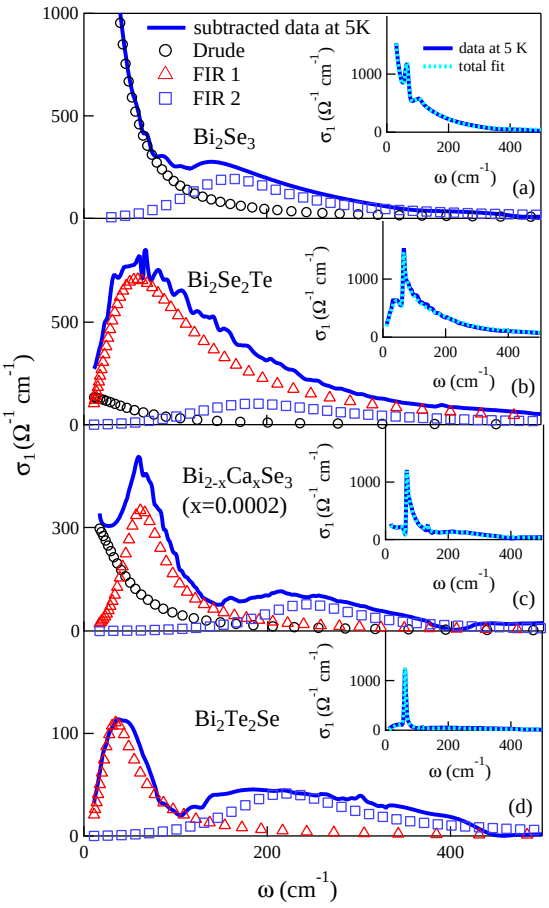

FIG. 3: (Color online) FIR optical conductivity at 5 K of the four Bi-based single crystals, after subtraction of both the interband and phonon contributions *via* Drude-Lorentz fits. The Drude term and the FIR contributions 1 and 2 are indicated by open circles, triangles, and squares, respectively. Note the different vertical scale in each panel.

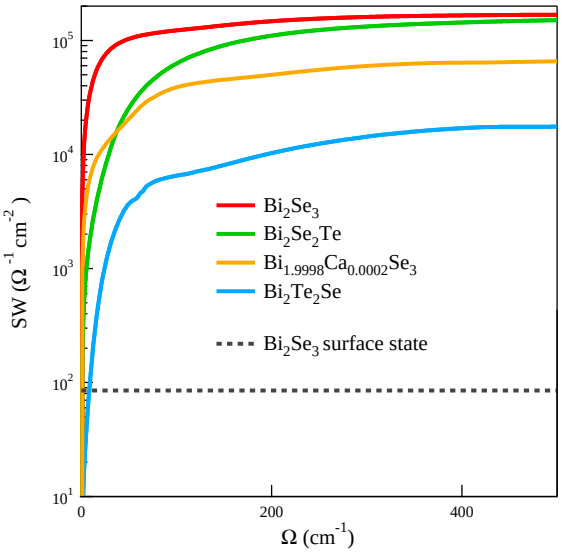

FIG. 4: (Color online) FIR spectral weight of all samples calculated at 5 K by Eq. 1. The dashed curve represents the contribution from the topological surface carriers as obtained from data of Refs. 35.

tinguished from the higher-frequency absorption. When crossing the IMT the low-frequency band transforms into a Drude term, while the high-frequency absorption persists in the metallic phase, indicating that the IMT occurs in an impurity band. [32] Therefore, in analogy with Si:P, the FIR2 band at 200 cm^{-1} in $Bi_{1.9998}Ca_{0.0002}Se_3$ and Bi_2Te_2Se can be assigned to the transitions from the impurity bound states to the electronic continuum. The FIR2 band is also in very good agreement with the impurity ionization energy estimated from the T-dependence of resistivity and Hall data, namely $E_i \sim$ 20-40 meV.[23, 24, 34] Instead, the low-frequency FIR1 band, clearly resolved both in $Bi_{1.9998}Ca_{0.0002}Se_3$ and Bi_2Te_2Se as shown in Figs. 3-c and -d, respectively, can be associated with hydrogen-like $1s \rightarrow np$ transitions, broadened by the inhomogeneous environment of the impurities and/or by their interactions. The spectra in Fig. 3 clearly show that, even in the most compensated topological insulator here measured, *i.e.* Bi_2Te_2Se, the FIR conductivity is still affected by extrinsic charge-carriers due to non-stoichiometry and doping.

A more quantitative comparison between the charge density expected for the topological surface states and that provided by extrinsic charge carriers can be obtained by calculating the optical spectral weight $SW(\Omega)$:

$$SW(\Omega) = \int_0^{\Omega} \sigma_1^{sub}(\omega)\mathrm{d}\omega \qquad (1)$$

where Ω=500 cm^{-1} is a cut-off frequency which well separates (see Fig.3) the low-frequency excitations from the interband transitions. In Fig. 4 one observes a decrease in the spectral weight by one order of magnitude from Bi_2Se_3 to Bi_2Te_2Se. This quantitatively shows the drastic effect of chemical compensation. From the previous SW one can estimate a 3D charge density n for Bi_2Se_3 of about 3 x 10^{18}/cm^3, which becomes $\sim 10^{17}$/cm^3 for Bi_2Te_2Se. This value agrees very well with the range 5 x 10^{16}-2 x 10^{17}/cm^3 extracted from transport measurements in crystals of the same batch.[25]

Recently, the THz conductivity of Bi_2Se_3 films grown by Molecular Beam Epitaxy (MBE) has been measured by a time-domain technique from 200 GHz to about 2 THz.[35, 36] The optical conductivity in this spectral region can be satisfactorily fit by a 2D Drude term plus the α phonon mode. The 2D Drude contribution has been associated to topological surface states.[35, 36] Therefore their spectral weight can be estimated from the Drude

plasma frequency (ω_{SSp}) as obtained from the fit in Refs. 35: $SW_{SS} = \omega^2_{SSp}/8$. This value is plotted in Fig. 4 by the dashed line. The actual SW in Bi_2Te_2Se is still higher, by nearly two orders of magnitude, than that expected from the topological surface states. This result indicates that the low-energy electrodynamics in single crystals of topological insulators, even at the highest degree of compensation presently achieved, and at the lowest temperatures where infrared spectra are taken, is still influenced by 3D charge excitations. Therefore, further improvements in the compensation are needed before bulk techniques like infrared spectroscopy may observe in single crystals the optical properties of purely topological metallic states.

We acknowledge the Helmholtz-Zentrum Berlin - Electron storage ring BESSY II for provision of synchrotron radiation at beamline IRIS. The research leading to these results has received funding from the European Community's Seventh Framework Programme (FP7/2007-2013) under grant agreement n.226716. The crystal growth was supported by the US national Science Foundation, grant DMR-0819860.

[1] M. Z. Hasan and C. L. Kane, Rev. Mod. Phys. **82**, 3045 (2010).
[2] C. L. Kane and E. J. Mele, Phys. Rev. Lett. **95**, 226801 (2005).
[3] J. E. Moore, Nature **464**, 194 (2010).
[4] L. Fu and C. L. Kane, Phys. Rev. Lett. **100** 096407 (2008).
[5] A. R. Akhmerov, J. Nilsson, and C.W.J. Beenakker, Phys. Rev. Lett. **102** 216404 (2009).
[6] X. -L. Qi, T.L. Hughes, and S.C. Zhang, Phys. Rev. B **78**, 195424 (2008).
[7] A. M. Essin, J.E. Moore, and D. Vanderbilt, Phys. Rev. Lett. **102** 146805 (2009).
[8] L. Fu and G. P. Collins, Sci. Am. **294**, 57(2006).
[9] A. Kitaev and J. Preskill Phys. Rev. Lett. **96**, 110404 (2006).
[10] X. Zhang, ,J. Wang, and S.C. Zhang, Phys. Rev. B **82**, 245107 (2010).
[11] Y. L. Chen, J. G. Analytis, J.-H. Chu, Z. K. Liu, S.-K. Mo, X. L. Qi, H. J. Zhang, D. H. Lu, X. Dai, Z. Fang, S. C. Zhang, I. R. Fisher, Z. Hussain, and Z.-X. Shen, Science **325**, 178 (2009).
[12] D. Hsieh, D. Qian, L. Wray, Y. Xia, Y. S. Hor, R. J. Cava, and M. Z. Hasan, Nature **452**, 970 (2008).
[13] H. Zhang, C. -X. Liu, X. -L. Qi, X. Dai, Z. Fang, and S.-C. Zhang, Nature Physics **5**, 438 (2009).
[14] Y. Xia, D. Qian, D. Hsieh, L. Wray, A. Pal, H. Lin, A. Bansil, D. Grauer, Y. S. Hor, R. J. Cava, and M. Z. Hasan, Nature Physics **5**, 398 (2009).
[15] Dong-Xia Qu, Y. S. Hor, Jun Xiong, R. J. Cava, and N. P. Ong, Science **329**, 821 (2010).
[16] A. D. La Forge, A. Frenzel, B. C. Pursley, Tao Lin, Xinfei Liu, Jing Shi, and D. N. Basov, Phys. Rev. B **81**, 125120 (2010).
[17] N. P. Butch, K. Kirshenbaum, P. Syers, A. B. Sushkov, G. S. Jenkins, H. D. Drew, and J. Paglione ,Phys. Rev. B **81**, 241301 (2010) .
[18] Y. S. Hor A. Richardella, P. Roushan, Y. Xia, J. G. Checkelsky, A. Yazdani, M. Z. Hasan, N. P. Ong, and R. J. Cava, Phys. Rev. B **79**, 195208 (2009).
[19] E. M. Black, E. M. Conwell, L. Seigle, C. W. spence Phys. Chem. Sol. **2**, 240 (1957).
[20] W. Richter, H. Köler, and C. R. Becker, Phys. Stat. Sol. (b) **84**, 619 (1977).
[21] H. Zhang, C. -X. Liu, X. -L. Qi, X. Dai, Z. Fang and S. -C. Zhang, Nat. Phys. **5**, 438 (2009).
[22] G. A. Thomas, D. H. Rapkine, R. B. Van Dover, L. F. Mattheiss, W. A. Sunder, L. F. Schneemeyer, and J. V. Waszczak , Phys. Rev. B **46**, 1553 (1992).
[23] Zhi Ren, A.A. Taskin, S. Sasaki, K. Segawa, and Y. Ando, Phys. Rev. B **82**, 241306(R) (2010)
[24] J. Xiong, Y. Luo, Y. Khoo, S. Jia, R. J. Cava, and N. P. Ong, Physica E: Low-dimensional Systems and Nanostructures **44** 5 920 (2012)
[25] Shuang Jia Huiwen Ji, E. Climent-Pascual, M. K. Fuccillo, M. E. Charles, Jun Xiong, N. P. Ong, and R. J. Cava, Phys. Rev. B **84**, 235206 (2011).
[26] R. J. Cava, private communication.
[27] M. Abo-Bakr, J. Feikes, K. Holldack, P. Kuske, W. B. Peatman, U. Schade, and G. Wustefeld , Phys. Rev. Lett. **90**, 094801 (2003).
[28] D. L. Greenaway and G. Harbeke, J. Phys. Chem. Solids **26**, 1585 (1965).
[29] A. Damascelli, K. Schulte, D. van der Marel, and A.A. Menovsky, Phys. Rev. B **55**, R4863 (1997).
[30] S. Lupi, M. Capizzi, P. Calvani, B. Ruzicka, P. Maselli, P. Dore, and A. Paolone , Phys. Rev. B **57**, 1248 (1998).
[31] G.A. Thomas, M. Capizzi, F. DeRosa, R. N. Bhatt, and T. M. Rice Phys. Rev. B **23**, 5472 (1981).
[32] A. Gaymann, H.P. Geserich, and H.v. Lohneysen, Phys. Rev. B **52** 16486 (1995).
[33] N. F. Mott, Metal-Insulator transitions, Taylor and Francis, London (1990).
[34] Y. S. Kim, M. Brahlek, N. Bansal, E. Edrey, G. A. Kapilevich, K. Iida, M. Tanimura, Y. Horibe, S. -W. Cheong, and S. Oh, Phys. Rev. B **84**, 073109 (2011).
[35] R. Valdés Aguilar, A. V. Stier, W. Liu, L. S. Bilbro, D. K. George, N. Bansal, L. Wu, J. Cerne, A. G. Markelz, S. Oh, and N. P. Armitage, Phys. Rev. Lett. **108**, 087403 (2012).
[36] R. Valdés Aguilar, L. Wu, A. V. Stier, L. S. Bilbro, M. Brahlek, N. Bansal, S. Oh, and N. P. Armitage arXiv:1202.1249.